Numerical investigation of wing crack initiation and propagation due to shear slip

Hau Trung Dang[1], Eirik Keilegavlen[1], Inga Berre[1,2].

[1] Department of Mathematics, University of Bergen, Bergen, Norway

[2] NORCE, Bergen, Norway

Hau.Dang@uib.no

Keywords: Geothermal system, wing crack, fracture propagation, shear slip, adaptive remeshing technique.

ABSTRACT

The expansion of wing cracks produced by slip of fractures due to water injection at pressure far below the minimum principal stress affects the performance of geothermal system. This work investigates how the wing cracks are emerged, propagated and connected due to slip at the interfaces of a pre-existing fracture. A mathematical model is presented and followed by an adaptive remeshing technique for the simulation. Several numerical investigations are conducted to validate the present model and study the initiation and propagation of wing cracks.

1. INTRODUCTION

An enhanced geothermal system (EGS) is a volume of hot rock that has been stimulated by reactivating natural fractures in the subsurface. By water injection at low pressure, slip is caused if the reduction in normal stress is sufficient to overcome the frictional resistance to the shear stresses on the fracture. The slip of fracture surfaces in opposite directions can cause the fracture to propagate in the form of wing crack (Cheng et al. 2019; Jung 2013; Kamali and Ghassemi 2016; Lin et al. 2010). In a system of multiple pre-existing natural fractures, many wing cracks are created and filled by massive water injection during stimulation. Some of them result in new connected flow paths and enhance permeability (Norbeck et al. 2018). While the propagation of wing crack could be central in stimulation of geothermal reservoirs, the mechanism has been only to a limited extent been studied by mathematical modeling and simulation in this context. Further improvements in modeling and simulation, will lead to increased understanding of this mechanism, while predictions will still be challenging due to the uncertainties in initial stress acting on the natural fractures as well as their locations (Lin et al. 2010). This leads to the lack of knowledge about the mechanism of wing cracks in EGS.

Many studies about behaviours of wing cracks in specimens made of rock/rock-like materials have been published, both related to experimental observations (Abdollahipour and Fatehi Marji 2016; Ashby and Hallam 1986; Bobet and Einstein 1998; Haeri et al. 2014; Horii and Nemat-Nasser 1985; Ingraffea and Manu 1980; Janeiro and Einstein 2010; Lee and Jeon 2011; Li et al. 2005; Park and Bobet 2009; Park and Bobet 2010; Shen et al. 1995; Wong and Einstein 2009; Xu et al. 2018; Yang et al. 2009; Yang 2011) and mathematical modeling (Bryant and Sun 2018; Fatehi Marji 2014; Gonçalves da Silva and Einstein 2013; Haeri et al. 2013; Ingraffea and Heuze 1980; Li and Wong 2012; Sharafisafa and Nazem 2014; Sivakumar and Maji 2016; Xie et al. 2016; Zhang et al. 2017). In these experiments, it is observed that emerging wing cracks at the tips of pre-existing fractures tend to align with the direction of the maximum compressive stress. By mathematical modeling, the behaviour of wing cracks in brittle material is usually modeled by use of the stress intensity factors (Lehner and Kachanov 1996) and/or a fracture criteria (Erdogan and Sih 1963; Hussain et al. 1973; Sih 1974). The maximum tangential stress (MTS) criterion seems to be the best choice for wing crack modeling because of the simplification and agreement with the observed trajectories (Gonçalves da Silva and Einstein 2013; Ingraffea and Heuze 1980). All these studies focused on the formation, growth and connection of wing cracks under external compressive load, as is relevant for EGS applications.

An inherent problem in simulation of fracture propagation is the disparate lengths scales involved: While the simulation domain can be quite large – in an EGS setting the reservoir is commonly measured in at least hundreds of meters - the fracturing processes takes place on a scale that is several of orders of magnitude smaller. Moreover, most numerical methods for fracture propagation are dependent on resolving the fracture in the grid, however, the fracture path is not known *a priori*. A possible remedy for both these issues is to apply adaptive remeshing (ARM) techniques to refine and adjust the mesh around an advancing fracture path.

This paper aims to present the mathematical model and an ARM technique conjunction with finite element method to understand how do wing cracks emerge, propagate and connect in a 2D-EGS model due to slip of pre-existing fracture interfaces. First, in section 2, the mathematical model for a wing crack was formulated based on linear elasticity theory, in combination with the MTS criterion. The displacement at interfaces of the pre-existing fracture is assumed to enforce a jump condition on displacement along the fracture. In section 3, a novel ARM technique that based on a simple error estimator, a deleted-displace process and Laplacian smoothing is proposed. The discretization will be presented in section 4. Several examples are discussed in section 5, in comparison with experiment data to validate and show the accuracy of the proposed model and procedure. Then a physical model is attempted to understand the role of wing cracks in shear stimulation of fractured geothermal reservoirs EGS.

2. GOVERNING EQUATIONS

Here we give the governing equations for the deformation of a linearly elastic medium, with emphasis on conditions placed on the boundaries of existing and newly created fractures. We also describe the criterion used to decide when and where a fracture will propagate.

2.1 Elasticity

Consider a plane strain domain $\Omega \subset \mathbb{R}^2$ with outward unit normal vector $\mathbf{n}$ on its boundary and a pre-existing fracture with boundary denoted by Γ_c as shown in Figure 1. The Dirichlet and Neumann conditions are applied on $\Gamma_{\mathrm{D}} \subset \Omega$ and $\Gamma_{\mathrm{N}} \subset \Omega$, respectively. For a linear elastic fracture problem, the strong form of governing equations can be expressed as

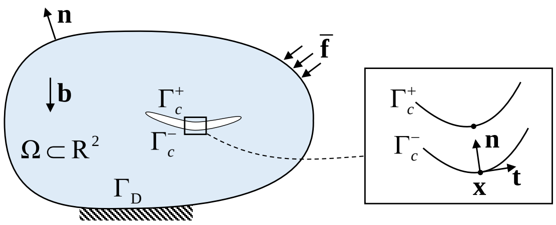

Figure 1: An elastic body containing a pre-existing fracture.

$$\begin{cases} \nabla \cdot \boldsymbol{\sigma} + \mathbf{b} = 0 & \text{in } \Omega \quad \text{Equilibrium eq.} \\ \boldsymbol{\sigma} = \mathbf{C} : \boldsymbol{\varepsilon} & \text{in } \Omega \quad \text{Constitutive eq.} \\ \boldsymbol{\varepsilon} = \frac{1}{2}\left(\nabla \mathbf{u} + \nabla \mathbf{u}^{\mathrm{T}}\right) & \text{in } \Omega \quad \text{Kinematic eq.} \\ \mathbf{u} = \bar{\mathbf{u}} & \text{on } \Gamma_{\mathrm{D}} \quad \text{Dirichlet BC} \\ \boldsymbol{\sigma} \cdot \mathbf{n} = \bar{\mathbf{f}} & \text{on } \Gamma_{\mathrm{N}} \quad \text{Neumann BC} \end{cases} \qquad [1]$$

where $\boldsymbol{\sigma}$, $\boldsymbol{\varepsilon}$ and $\mathbf{u}$ are the Cauchy stress tensor, the symmetric infinitesimal strain tensor and the displacement field, respectively. $\mathbf{C}$ is the fourth-order elasticity (Hooke's) tensor defined from Young's modulus, E, and Poisson's ratio, v. $\mathbf{b}$ is the body force. $\bar{\mathbf{u}}$ and $\bar{\mathbf{f}}$ are the prescribed displacement along the Dirichlet boundary and the applied traction along the Neumann boundary, respectively.

When a pre-existing fracture Γ_c is compressed and/or slipped, the normal jump displacement condition is imposed at the fractures' interfaces Γ_c^+ and Γ_c^-. As the focus in this work is on the effect of shear slip, it is for simplicity assumed that the normal fracture dilation is zero, i.e.,

$$[\mathbf{u}]_{\mathbf{n}}^{\Gamma_c} = \left[\mathbf{u}^{\Gamma_c^+}(\mathbf{x}) - \mathbf{u}^{\Gamma_c^-}(\mathbf{x})\right] \cdot \mathbf{n}(\mathbf{x}) = 0 \qquad [2]$$

For the tangential direction of Γ_c, two types of conditions are considered: Either, the fracture surfaces are modeled as frictionless, thus the tangential traction is zero at Γ_c,

$$\boldsymbol{\sigma} \cdot \mathbf{t} = 0 \qquad [3]$$

where $\mathbf{t}$ is the tangential vector on the surfaces of a pre-existing fracture. This assumption, in practice, leads to an exaggeration of the slip, but is acceptable herein, as the trajectory of fracture is the primary quantity of interest. For the friction-free case, the deformation of the elastic medium and the fractures contained within is driven by external boundary conditions on Γ_{D} and Γ_{N}, or by displacements on other fractures.

The second type of condition considered in the tangential direction of Γ_c is a specified displacment jump i.e.,

$$[\mathbf{u}]_{\mathbf{t}}^{\Gamma_c} = \left[\mathbf{u}^{\Gamma_c^+}(\mathbf{x}) - \mathbf{u}^{\Gamma_c^-}(\mathbf{x})\right] \cdot \mathbf{t} = u_0' \qquad [4]$$

where the total slip at Γ_c, u_0', is considered as known. In the context of low-pressure stimulation of geothermal systems, this type of condition applies to sliding fractures.

The wing cracks emerged after compressed and/or slipped are the tensile cracks (Bobet and Einstein 1998; Wong and Einstein 2009). This means that the surfaces of this cracks are in not contact and both normal and tangential tractions at these faces are zeros, i.e.,

$$\boldsymbol{\sigma} \cdot \mathbf{n} = \boldsymbol{\sigma} \cdot \mathbf{t} = 0 \qquad [5]$$

The wing cracks are not present in the computational domain at the start of the simulations. Indeed, the computation of the time of fracturing and the paths of wing cracks is the main challenge in this work.

2.2 Fracture criteria

The primary mechanism for permeability enhancement in the construction of EGS systems is believed to be sliding of pre-existing fractures. This motion will alter the stress field in the rock surrounding rock matrix, and may trigger propagation of new fractures, commonly denoted wing cracks, emanating from the fracture tips. The modeling and computation of this secondary fracturing is of interest in this work.

From the mathematical model for elastic deformation, the stress at an arbitrary point can be directly calculated for a certain problem. So, the fracture criteria based on maximum tensile stress (MTS) (Erdogan and Sih 1963) that is simple and accuracy (Gonçalves da Silva and Einstein 2013; Ingraffea and Heuze 1980), should be adapted to predict the initiation and propagation of wing cracks in EGS. This criterion states that a crack grows when the maximum average tangential stress in the fracture process zone ahead of the crack tip reaches a critical value. Moreover, the crack growth direction coincides with the direction of the maximum average tangential stress along a constant radius around the crack tip. It is a local approach since it is based on local stress fields around the crack front. The tangential stress in around a crack tip is given by

$$\sigma_\theta = \frac{1}{\sqrt{2\pi l}}\left(K_I \cos^3\frac{\theta}{2} - \frac{3}{2}K_{II}\cos\frac{\theta}{2}\sin\theta\right) \qquad [6]$$

The wing crack emerges if the tangential stress reaches a critical value, i.e.

$$\sigma_{\theta_0}\sqrt{2\pi l} = K_I \cos^3\frac{\theta_0}{2} - \frac{3}{2}K_{II}\cos\frac{\theta_0}{2}\sin\theta_0 = K_{\mathrm{IC}} \qquad [7]$$

where K_{IC} is the fracture toughness, θ_0 is the crack initiation angle with respect to the original crack plane. θ_0 is obtained by solving $\partial\sigma_\theta / \partial\theta = 0$ for θ and combining with sufficient condition $\partial^2\sigma_\theta / \partial\theta^2 < 0$ such as

$$\theta_0 = 2\tan^{-1}\left(\frac{1}{4}\mu \pm \frac{1}{4}\sqrt{\mu^2+8}\right),\ \mu = K_I / K_{II} \qquad [8]$$

$$K_{II}\left(\sin\frac{\theta_0}{2} + 9\sin\frac{3\theta_0}{2}\right) < K_I\left(\cos\frac{\theta_0}{2} + 3\cos\frac{3\theta_0}{2}\right) \qquad [9]$$

in which K_I and K_{II} are the stress intensity factors (SIFs), as parameters for the intensity of stresses close to the crack tip, can be evaluated by several techniques (Moran and Shih 1987; Parks 1974; Phongthanapanich and Dechaumphai 2004). In this work, SIFs are computed by the nodal displacement correlation technique (Parks 1974) in conjunction of collapsed quarter point singular elements (CQPE) (Barsoum 1976; Henshell and Shaw 1975). CQPEs considerably improve the numerical solution near the crack tip, result in more accurate computation of SIFs (Khoei et al. 2008). Through the displacement of CQPE around a crack tip, these SIFs can be calculated as

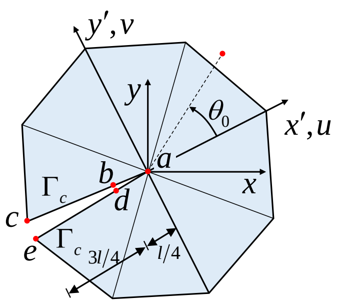

Figure 2: The collapsed quarter point singular elements around a crack tip.

$$\begin{aligned} K_I &= \frac{E}{12(1-\nu^2)}\sqrt{\frac{2\pi}{l}}\left[4(v'_b - v'_d) - \frac{1}{2}(v'_c - v'_e)\right] \\ K_{II} &= \frac{E}{12(1-\nu^2)}\sqrt{\frac{2\pi}{l}}\left[4(u'_b - u'_d) - \frac{1}{2}(u'_c - u'_e)\right] \end{aligned} \qquad [10]$$

where l is the crack tip rosette radius. u' and v' are the local displacements of nodal points located on the crack in CQPE, in which x' is aligned in the direction of crack axis, as shown in Figure 2.

3. DISCRETIZATION

The finite element discretization of the governing equations shown in the previous section are presented in this section, together with an adaptive remeshing technique. The propagation of wing cracks is complicated, and their trajectories are difficult to achieve by analytical approach. In this case numerical solutions by the finite element method (FEM) is a natural alternative. The finite element formulation is based on the weak formulation established from the governing equation and states: Find $\mathbf{u} \in V$ such that $\forall \mathbf{v} \in V$

$$\begin{aligned} &\int_\Omega \mathbf{u}^{\mathrm{T}}\mathbf{L}^{\mathrm{T}}\mathbf{D}\mathbf{L}\mathbf{v}\,\mathrm{d}\Omega - \int_{\Gamma_c} \boldsymbol{\sigma}\cdot\mathbf{n}[\mathbf{v}]_{\mathbf{n}}\,\mathrm{d}\Gamma \\ &= \int_\Omega \mathbf{b}\mathbf{v}\,\mathrm{d}\Omega + \int_{\Gamma_{\mathrm{N}}} \bar{\mathbf{f}}\mathbf{v}\,\mathrm{d}\Gamma \end{aligned} \qquad [11]$$

where $\mathbf{u}$ must be selected from a set of admissible functions in the space V such that

$$\mathbf{u} \in V := \left\{\mathbf{v} \in H^1(\Omega),\ \mathbf{v}|_{\Gamma_{\mathbf{u}}} = 0\right\} \qquad [12]$$

in which H^1 is the standard Sobolev space. In Eq. [11] $\mathbf{L}$ and $\mathbf{D}$ are the differential operator and the material matrix modified from $\mathbf{C}$ given by

$$\mathbf{L}^{\mathrm{T}} = \begin{bmatrix} \frac{\partial}{\partial x} & 0 & \frac{\partial}{\partial y} \\ 0 & \frac{\partial}{\partial y} & \frac{\partial}{\partial x} \end{bmatrix},\ \mathbf{D} = \frac{E}{1-\nu^2}\begin{bmatrix} 1 & \nu & 0 \\ \nu & 1 & 0 \\ 0 & 0 & \frac{1}{2}(1-\nu) \end{bmatrix} \qquad [13]$$

3.1 Finite element method

The approximate solution of Eq. [11], denoted by $\mathbf{u}_h$, can be evaluated by using a subset of the allowable function space $V_h \subset V$ composed of first order Lagrangian shape functions, that is, piecewise linear functions. This requires discretizing the domain Ω into m non-overlapping finite elements that conform to the fracture geometry, such that

$$\Omega \cong \Omega^h \equiv \bigcup_{e=1}^{m} \Omega_e \qquad [14]$$

where Ω_e are triangular elements in this work. For each element Ω_e, the displacement field is approximated as a linear function, which is expressed in terms of the displaced values at the three vertices such that

$$\mathbf{u} = \begin{Bmatrix} u \\ v \end{Bmatrix} \cong \begin{Bmatrix} N_i u_i \\ N_i v_i \end{Bmatrix} = \mathbf{N}\mathbf{u}_h^e \qquad [15]$$

By substituting Eq. [15] into Eq. [11], the discretized system can be written as

$$\mathbf{K}\mathbf{u}_h = \mathbf{F} \qquad [16]$$

where $\mathbf{K}$ and $\mathbf{F}$ are the global stiffness matrix and global load vector, respectively. For elements that are not adjacent to a fracture surface, they are obtained by assembly from each element and expressed as follows

$$\mathbf{K} = \sum_{e=1}^{m} \mathbf{K}_e = \sum_{e=1}^{m} \int_{\Omega_e} \mathbf{B}^{\mathrm{T}} \mathbf{D} \mathbf{B} \mathrm{d}\Omega \qquad [17]$$

$$\mathbf{F} = \sum_{e=1}^{m} \mathbf{F}_e + \mathbf{F}_t = \sum_{e=1}^{m} \int_{\Omega_e} \mathbf{N}^{\mathrm{T}} \mathbf{b} \mathrm{d}\Omega + \int_{\Gamma_t} \mathbf{N}^{\mathrm{T}} \bar{\mathbf{t}} \mathrm{d}\Gamma \qquad [18]$$

where $\mathbf{B}$ is gradient matrix defined as

$$\mathbf{B} = \mathbf{L}\mathbf{N} \qquad [19]$$

3.2 Adaptive remeshing technique

The accuracy of the FEM simulation depends on the quality of the mesh that is affected by the geometric discretization errors and the gradients of solution within individual elements. For the fracture propagation problem in a linearly elastic medium, the stress is singular at the fracture tip and drops quickly away from the fracture tip. In this work, we consider a combination of two techniques to give a reasonable representation of this behaviour in the vicinity of the crack tip: First mesh refinement based on an error estimation to improve the accuracy of FEM, and second, remeshing around crack tip domain by the collapsed quarter point elements to represent the tip singularity, and thus improve the accuracy in computation of the stress intensity factors and to easily extend crack in this domain. In addition, a third ingredient of our approach is Laplacian smoothing to improve the quality of the mesh.

4. NUMERICAL INVESTIGATION

In this section, three numerical examples are investigated. The first and second intended for validation purposes, while the last one is designed for EGS applications: To validate the proposed model, the propagation paths of wing cracks in domains with a single and two pre-existing fractures under uniaxial compression are considered and compared with experimental observations. After that, this model is extended to a more complex problem where the surfaces of one fracture slip and creates wing cracks that connects to other fractures.

4.1 Validation

The compression test of a rock specimen with a single pre-existing fracture as shown in Figure 3 is adapted. The fracture is inclined located at 45˚ to the horizontal direction at center of the specimen. The material parameters are Young's modulus E = 36.2 GPa, Poisson's ratio ν = 0.21, fracture toughness K_{IC} = 6.5 MPa·m$^{1/2}$. The size of specimen is 102 × 102 mm^2 and of the length of fracture is 20.32 mm. Boundary conditions on the specimen are indicated in Figure 3; on the existing fracture, a no-friction condition is assigned in the tangential direction.

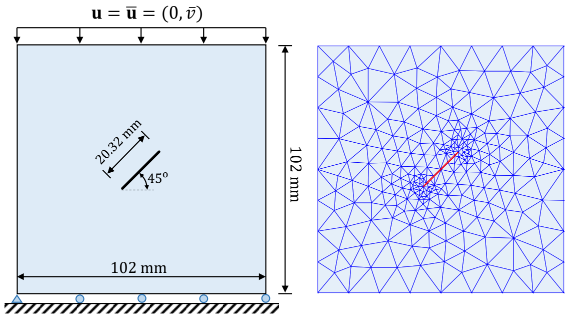

Figure 3: Geometry of specimen with a single pre-existing fracture.

The propagation paths of two wing cracks originated from tips of the pre-existing fracture is shown in Figure 4. The paths are curvilinear and tend to migrate of around 70 degrees and gradually turn in the loading direction. The trajectories of the wing cracks obtained in this work is similar to the observation from the experiments reported in (Ashby and Hallam 1986; Haeri et al. 2014; Ingraffea and Manu 1980; Lee and Jeon 2011; Shen et al. 1995).

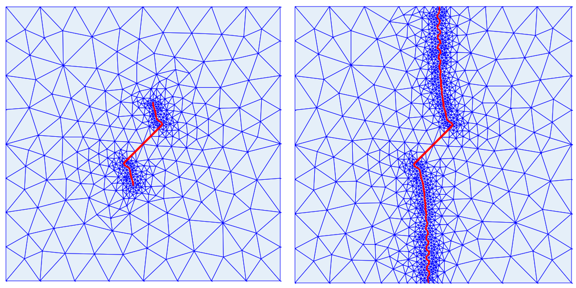

Figure 4: The trajectories of wing cracks from a single pre-existing crack.

As a second test, consider the connection of double pre-existing fractures in a specimen under the uniaxial compression. The specimen shown in Figure 5 is made from gypsum with the material parameters are as follows: Young's modulus E = 5.96 GPa, Poisson's ratio ν = 0.24, fracture toughness K_{IC} = 0.1778 MPa·m$^{1/2}$. The size of the specimen is 152.4 × 76.2 mm^2. There are two pre-existing fractures are in the specimen and inclined at 45˚ to the horizontal direction. Boundary conditions on the specimen are indicated in Figure 5; again, no-friction conditions are assigned in the tangential direction of the pre-existing fractures.

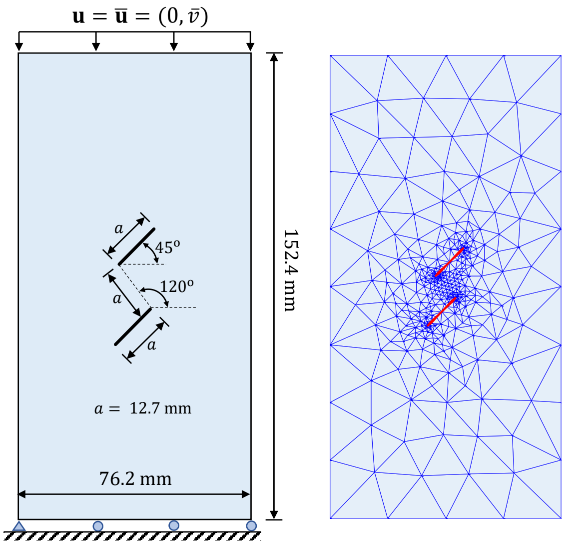

Figure 5: Geometry of a specimen with two pre-existing fractures.

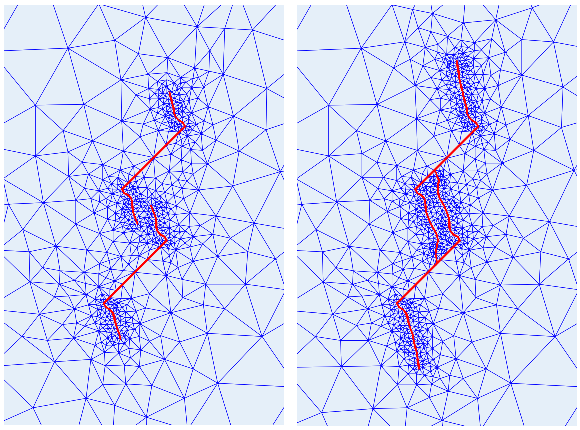

Figure 6: The trajectories of wing cracks from double pre-existing cracks

The fracture propagation process is shown in Figure 6. The wings cracks initiate at the two tips of each pre-existing fracture and propagate in opposite directions. Then the wing crack originating from one fracture links to other fractures to extend the failure. The trajectories of the wing cracks are curvilinear and similar to that observed previously in the compression test of the rock (Park and Bobet 2009; Shen et al. 1995).

The agreement with experimental observations in the above examples shows that the mathematical model proposed in this work is valid for the fracture propagation in type of wing cracks. Compared to a finely resolved static grid, the ARM technique significantly reduces the computational cost, while preserving accuracy of the predicted fracture trajectory. Motivated by this confirmation, the procedure is extended to investigate a typical problem in EGS that wing cracks emerge and propagate not by compression stress but by sliding in opposite direction of interfaces of a pre-existing fracture. This extension is presented in the next example.

4.2 EGS application

This example extends the proposed model to the problem of enhanced permeability in EGS. The example setup and geometry are shown in Figure 7, in which three natural horizontal fractures exist initially in a specimen. The size and length of the specimen and fractures are, respectively, 3000×2000 mm^2 and 500 mm. The material parameters are the same as for first example. A measurable slip is imposed on the middle fracture, mimicking the slip due to water injection in fracture shear stimulation. Instead of compressive stress, the slip is considered the cause of wing cracks in EGS.

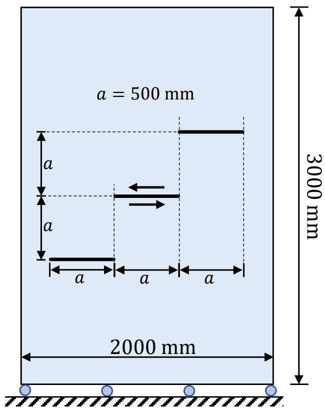

Figure 7: Geometry of specimens with three pre-existing fractures.

The initiation and propagation of wing cracks are shown in Figure 8. When a pre-existing fracture experience a jump in tangential displacements, wing cracks may emerge at its tips, tend to migrate of around 70 degrees and gradually turn in the almost perpendicular directions. If the tectonic stress stored in this fracture is large enough, wing cracks propagate away and link to nearby fractures to form connected flow pathways. Then water flows to these fractures and the process of developing wing cracks is repeated to enhance permeability in EGS.

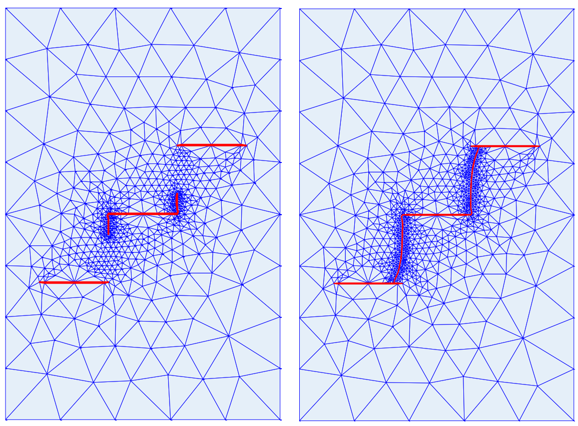

Figure 8: The trajectories of wing cracks caused by shear slip at interfaces a pre-existing crack

The obtained results in this example show that, the mechanism of wing cracks caused by the shear slip in the interfaces of a pre-existing fracture is predictable.

This is important for improving the performance of geothermal systems which are significantly influenced by permeability.

5. CONCLUSIONS

The simple mathematical model and the ARM technique are presented in this work to simulate the wing cracks initiation and propagation in rock material. The model is established based on the linear elasticity theory, in combination with MTS criterion. An ARM technique is developed based on a simple error estimator, deleted-replaced process and Laplacian smoothing. Three examples are considered. The first and second examples are for validation purposes, while the last one is designed to investigate the mechanism of wing cracks in EGS. The obtained results in this work show the accuracy and effectiveness of the proposed model and procedure in the prediction of wing cracks propagation caused by both compression and shear slip.

REFERENCES

Abdollahipour, A. and Fatehi Marji, M.: Analyses of Inclined Cracks Neighboring Two Iso-Path Cracks in Rock-Like Specimens Under Compression, *Geotechnical and Geological Engineering*, **35**, (2016), 169–181.

Ashby, M. F. and Hallam, S. D.: The failure of brittle solids containing small cracks under compressive stress states, *Acta Metallurgica*, **34**, (1986), 497–510.

Barsoum, R. S.: On the use of isoparametric finite elements in linear fracture mechanics, *International Journal for Numerical Methods in Engineering*, **10**, (1976), 25–37.

Bobet, A. and Einstein, H. H.: Fracture coalescence in rock-type materials under uniaxial and biaxial compression, *International Journal of Rock Mechanics and Mining Sciences*, **35**, (1998), 863–888.

Bryant, E. C. and Sun, W.: A mixed-mode phase field fracture model in anisotropic rocks with consistent kinematics, *Computer Methods in Applied Mechanics and Engineering*, **342**, (2018), 561–584.

Cheng, Q., Wang, X. and Ghassemi, A.: Numerical simulation of reservoir stimulation with reference to the Newberry EGS, *Geothermics*, **77**, (2019), 327–343.

Erdogan, F. and Sih, G. C.: On the Crack Extension in Plates Under Plane Loading and Transverse Shear, *Journal of Basic Engineering*, **85**, (1963), 519–525.

Fatehi Marji, M.: Numerical analysis of quasi-static crack branching in brittle solids by a modified displacement discontinuity method, *International Journal of Solids and Structures*, **51**, (2014), 1716–1736.

Gonçalves da Silva, B. and Einstein, H.: Modeling of crack initiation, propagation and coalescence in rocks, *International Journal of Fracture*, **182**, (2013), 167–186.

Haeri, H., Shahriar, K., Fatehi Marji, M. and Moarefvand, P.: A coupled numerical–experimental study of the breakage process of brittle substances, *Arabian Journal of Geosciences*, **8**, (2013), 809–825.

Haeri, H., Shahriar, K., Fatehi Marji, M. and Moarefvand, P.: Experimental and numerical study of crack propagation and coalescence in pre-cracked rock-like disks, *International Journal of Rock Mechanics and Mining Sciences*, **67**, (2014), 20–28.

Henshell, R. D. and Shaw, K. G.: Crack tip finite elements are unnecessary, *International Journal for Numerical Methods in Engineering*, **9**, (1975), 495–507.

Horii, H. and Nemat-Nasser, S.: Compression-induced microcrack growth in brittle solids: Axial splitting and shear failure, *Journal of Geophysical Research: Solid Earth*, **90**, (1985), 3105–3125.

Hussain, M. A., Pu, S. L. and Underwood, J.: Strain Energy Release Rate for a Crack Under Combined Mode I and Mode II, *Proceedings of the National Symposium on Fracture Mechanics 1973*, Washington, USA, (1973), paper #001, 2-28.

Ingraffea, A. R. and Heuze, F. E.: Finite element models for rock fracture mechanics, *International Journal for Numerical and Analytical Methods in Geomechanics*, **4**, (1980), 25–43.

Ingraffea, A. R. and Manu, C.: Stress-intensity factor computation in three dimensions with quarter-point elements, *International Journal for Numerical Methods in Engineering*, **15**, (1980), 1427–1445.

Janeiro, R. P. and Einstein, H. H.: Experimental study of the cracking behavior of specimens containing inclusions (under uniaxial compression), *International Journal of Fracture*, **164**, (2010), 83–102.

Jung, R.: EGS — Goodbye or Back to the Future, in: Effective and Sustainable Hydraulic Fracturing, Rob, J. (Ed.) 95–121, *INTECH*, (2013).

Kamali, A. and Ghassemi, A.: Analysis of Natural Fracture Shear Slip and Propagation in Response to Injection, *Proceeding of the 41st Workshop on Geothermal Reservoir Engineering 2016*, California, USA, (2016), paper #050, 584-593.

Khoei, A. R., Azadi, H. and Moslemi, H.: Modeling of crack propagation via an automatic adaptive mesh refinement based on modified superconvergent patch recovery technique, *Engineering Fracture Mechanics*, **10**, (2008), 2921–2945.

Lee, H. and Jeon, S.: An experimental and numerical study of fracture coalescence in pre-cracked specimens under uniaxial compression, *International Journal of Solids and Structures*, **48**, (2011), 979–999.

Lehner, F. and Kachanov, M.: On modelling of 'winged" cracks forming under compression, *International Journal of Fracture*, **77**, (1996), 69–75.

Li, H. and Wong, L.: Influence of flaw inclination angle and loading condition on crack initiation and propagation, *International Journal of Solids and Structures*, **49**, (2012), 2482–2499.

Li, Y.-P., Chen, L.-Z. and Wang, Y.-H.: Experimental research on pre-cracked marble under compression, *International Journal of Solids and Structures*, **42**, (2005), 2505–2516.

Lin, W., Yeh, E.-C., Hung, J.-H., Haimson, B. and Hirono, T.: Localized rotation of principal stress around faults and fractures determined from borehole breakouts in hole B of the Taiwan Chelungpu-fault Drilling Project (TCDP), *Tectonophysics*, **482**, (2010), 82–91.

Moran, B. and Shih, C. F.: A general treatment of crack tip contour integrals, *International Journal of Fracture*, **35**, (1987), 295–310.

Norbeck, J. H., McClure, M. W. and Horne, R. N.: Field observations at the Fenton Hill enhanced geothermal system test site support mixed-mechanism stimulation, *Geothermics*, **74**, (2018), 135–149.

Park, C. H. and Bobet, A.: Crack coalescence in specimens with open and closed flaws: A comparison, *International Journal of Rock Mechanics and Mining Sciences*, **46**, (2009), 819–829.

Park, C. H. and Bobet, A.: Crack initiation, propagation and coalescence from frictional flaws in uniaxial compression, *Engineering Fracture Mechanics*, **77**, (2010), 2727–2748.

Parks, D. M.: A stiffness derivative finite element technique for determination of crack tip stress intensity factors, *International Journal of Fracture*, **10**, (1974), 487–502.

Phongthanapanich, S. and Dechaumphai, P.: Adaptive Delaunay triangulation with object-oriented programming for crack propagation analysis, *Finite Elements in Analysis and Design*, **40**, (2004), 1753–1771.

Sharafisafa, M. and Nazem, M.: Application of the distinct element method and the extended finite element method in modelling cracks and coalescence in brittle materials, *Computational Materials Science*, **91**, (2014), 102–121.

Shen, B., Stephansson, O., Einstein, H. H. and Ghahreman, B.: Coalescence of fractures under shear stresses in experiments, *Journal of Geophysical Research: Solid Earth*, **100**, (1995), 5975–5990.

Sih, G. C.: Strain-energy-density factor applied to mixed mode crack problems, *International Journal of Fracture*, **10**, (1974), 305–321.

Sivakumar, G. and Maji, V.: Simulation of crack propagation in rocks by XFEM, *Proceedings of the conference on Recent Advances in Rock Engineering 2016*, Karnataka, India, (2016), paper #046.

Wong, L. N. Y. and Einstein, H. H.: Systematic evaluation of cracking behavior in specimens containing single flaws under uniaxial compression, *International Journal of Rock Mechanics and Mining Sciences*, **46**, (2009), 239–249.

Xie, Y., Cao, P., Liu, J. and Dong, L.: Influence of crack surface friction on crack initiation and propagation: A numerical investigation based on extended finite element method, *Computers and Geotechnics*, **74**, (2016), 1–14.

Xu, J., Zheng, Z., Xiao, X. and Li, Z.: Crack propagation and coalescence due to dual non-penetrating surface flaws and their effect on the strength of rock-like material, *Journal of Geophysics and Engineering*, **15**, (2018), 938–951.

Yang, S. Q.: Crack coalescence behavior of brittle sandstone samples containing two coplanar fissures in the process of deformation failure, *Engineering Fracture Mechanics*, **78**, (2011), 3059–3081.

Yang, S. Q., Dai, Y. H., Han, L. and Q. Jin, Z.: Experimental study on mechanical behavior of brittle marble samples containing different flaws under uniaxial compression, *Engineering Fracture Mechanics*, **76**, (2009), 1833–1845.

Zhang, X., Sloan, S., Vignes, C. and Sheng, D.: A modification of the phase-field model for mixed mode crack propagation in rock-like materials, *Computer Methods in Applied Mechanics and Engineering*, **322**, (2017), 123–136.

Acknowledgements

This work was funded by the ERiS project, grant #267909, Research Council of Norway.